Simulation of atomic layer deposition on nanoparticle agglomerates

Jin, Wenjie; van Ommen, Ruud; Kleijn, Chris

DOI
10.1116/1.4968548

Publication date
2016

Document Version
Final published version

Published in
Journal of Vacuum Science and Technology. Part A: International Journal Devoted to Vacuum, Surfaces, and Films

Simulation of atomic layer deposition on nanoparticle agglomerates

Wenjie Jin, Chris R. Kleijn, and J. Ruud van Ommen

Citation: Journal of Vacuum Science & Technology A: Vacuum, Surfaces, and Films **35**, 01B116 (2017); doi: 10.1116/1.4968548

View online: http://dx.doi.org/10.1116/1.4968548

View Table of Contents: http://avs.scitation.org/toc/jva/35/1

Published by the American Vacuum Society

Simulation of atomic layer deposition on nanoparticle agglomerates

Wenjie Jin,[a] Chris R. Kleijn, and J. Ruud van Ommen
Department of Chemical Engineering, Delft University of Technology, van der Maasweg 9, 2629 HZ Delft, The Netherlands

(Received 12 September 2016; accepted 10 November 2016; published 29 November 2016)

Coated nanoparticles have many potential applications; production of large quantities is feasible by atomic layer deposition (ALD) on nanoparticles in a fluidized bed reactor. However, due to the cohesive interparticle forces, nanoparticles form large agglomerates, which influences the coating process. In order to study this influence, the authors have developed a novel computational modeling approach which incorporates (1) fully resolved agglomerates; (2) a self-limiting ALD half cycle reaction; and (3) gas diffusion in the rarefied regime modeled by direct simulation Monte Carlo. In the computational model, a preconstructed fractal agglomerate of up to 2048 spherical particles is exposed to precursor molecules that are introduced from the boundaries of the computational domain and react with the particle surfaces until these are fully saturated. With the computational model, the overall coating time for the nanoparticle agglomerate has been studied as a function of pressure, fractal dimension, and agglomerate size. Starting from the Gordon model for ALD coating within a cylindrical hole or trench [Gordon *et al.*, Chem. Vap. Deposition **9**, 73 (2003)], the authors also developed an analytic model for ALD coating of nanoparticles in fractal agglomerates. The predicted coating times from this analytic model agree well with the results from the computational model for $D_f = 2.5$. The analytic model predicts that realistic agglomerates of $O(10^9)$ nanoparticles require coating times that are 3–4 orders of magnitude larger than for a single particle. © *2016 American Vacuum Society*. [http://dx.doi.org/10.1116/1.4968548]

I. INTRODUCTION

Modifying the surface of nano- and micron-sized particles results in new functionalities that have applications in many diverse fields, such as catalysis, medicine, and energy conversion and storage.[1–4] Atomic layer deposition (ALD) is one such technique that can tune the particle surface by depositing precisely controlled thin film layers. It relies on two self-limiting surface reactions applied in an alternating sequence, which allows for atomic control over the film thickness and composition.[5] ALD coating on nanoparticles has been demonstrated in several experimental studies utilizing a fluidized bed.[6,7] In fluidized bed ALD, an amount of particles is suspended in an upward gas stream containing the precursor molecules. It is a useful technique for large scale processing of particles. However, when fluidizing nanoparticles, they form agglomerates with sizes up to a few hundred microns due to the cohesive interparticle forces. These agglomerates are (highly) porous, and their complex geometries have been commonly described as fractal for their self-similarity under different length scales.[8–10] Typical fractal dimensions have been found to range from 1.8 to 2.7. When applying ALD to such agglomerates of nanoparticles, the precursor molecules need to be transported into the porous agglomerates and then react with the particle surfaces. This introduces a time scale for the gas transport which may influence the overall coating time. A good understanding of this phenomenon is important for the optimization of the ALD process cycles and an efficient utilization of the precursors.[11]

Reaction–diffusion problems in porous media, such as catalyst particles, polymer networks, and particle assemblies, have been studied for many decades following the seminal work by Thiele.[12] There now exists an extensive body of literature[13–21] addressing reaction–diffusion in porous media for various types of reactions (e.g., homogeneous and heterogeneous reactions, first- and nonfirst order reactions), various treatments of the porous structure geometry (e.g., by treating the porous structure as a single material with an effective diffusivity, or by explicitly taking into account the geometric details of the pores) and various pore geometries (e.g., cylindrical pores, packed beds). For gases, another distinction is that between the molecular diffusion regime (when the typical length scale L of the pores is much larger than the mean free path λ of the gas molecules, or the Knudsen number $Kn = \lambda/L \ll 1$), the free molecular regime ($Kn \gg 1$) and the transitional or the Knudsen diffusion regime ($0.1 < Kn < 10$). For ALD coating of nanoparticle agglomerates, depending on the operating pressure, it is generally necessary to account for gas rarefaction as the mean free path can be comparable to or larger than that of the particles and the pores ($\lambda \sim 10 - 100$ nm for atmospheric pressure, and $\lambda \sim 10 - 100$ μm for 1 mbar).

Reaction–diffusion problems in particle agglomerates have been studied for numerically generated agglomerates constructed from an assembly of particles with predefined assembling rules.[22–25] However, some of these studies only focus on the molecular diffusion regime ($Kn \ll 1$),[22–24] whereas others do not address self-limiting reactions in fractal geometries.[22–25] On the other hand, self-limiting ALD reactions and rarefied gas diffusion have been studied inside very simple pore geometries such as narrow trenches and cylindrical pores.[26–28]

[a]Electronic mail: W.Jin-1@tudelft.nl

In the present paper, we develop and demonstrate a computational model for the rarefied reaction–diffusion problem in ALD coating of agglomerated nanoparticles which, in deviation from all previous studies, combines models for (1) a fully resolved fractal agglomerate; (2) self-limiting half cycle ALD reactions; and (3) diffusion in the transition regime. Each of these aspects has been studied in literature, but to the best of our knowledge, the combination of these three is novel. With our computational model, the overall coating time is studied, focusing on the influence of pressure, agglomerate size, and agglomerate fractal dimension. We also present an analytic model which predicts the scaling of the coating time with agglomerate size, allowing for the extrapolation of our results to realistically large agglomerates.

A. Numerical construction of fractal agglomerates

It is commonly agreed in literature[8,29] that a fractal agglomerate can be characterized by its size and fractal dimension as

$$N = k_f \left(\frac{R_g}{a}\right)^{D_f}, \tag{1}$$

where N is the total number of particles in an agglomerate, k_f is a constant prefactor, a is the radius of the primary particle, and R_g is the size of the agglomerate which is often represented by its gyration radius.

Filippov *et al.*[30] first proposed a tunable algorithm to numerically generate agglomerates which exactly fulfil Eq. (1) for any given combination of N, k_f and D_f. Skorupski *et al.*[31] further improved this algorithm and developed a fast computational implementation. In this work, we have implemented the improved algorithm by following Skorupski *et al.* Figure 1 gives examples of the constructed fractal agglomerate with different D_f. Note that an increase in fractal dimension leads to a more dense structure of the agglomerate.

B. Direct simulation Monte Carlo

Direct simulation Monte Carlo (DSMC)[32] is a well-developed and widely applied technique for simulating rarefied gas flows, such as in aerodynamics in aerospace applications[33] and in microscale devices.[34,35] In DSMC, the gas molecules are represented by so called DSMC parcels, with each parcel representing a large number N_{eq} of real molecules. These parcels move and collide with each other in the simulated physical space. One essential feature of DSMC is the decoupling between the parcel motion and parcel–parcel collisions over a sufficiently small time interval. Upon collision, the parcels interchange momentum and energy according to a given collision model. Earlier work has extensively shown that DSMC gives a good representation of real rarefied gas flows.[36] For our model, we have chosen the variable soft sphere (VSS)[32] collision model for its accuracy in reproducing both the viscosity and diffusivity for the gas mixture.

C. Modeling ALD surface reaction

In reality, the ALD surface chemistry is rather complex, including nonideal ALD behaviors, such as the readsorption of gaseous products[37] and non-self-limiting behavior due to the decomposition of the surface species.[5] However, the aim of this work is to study the influence of fractal structure and gas rarefaction on the overall coating time. Therefore, here we adopt the ideal self-limiting ALD model based on the widely used concept of sticking coefficient. The sticking coefficient is defined as the reaction probability of a single precursor molecule with a reactive site on the surface. In order to mimic the self-limiting behavior, we use a similar methodology as adopted in earlier publications,[26–28] based on the surface book-keeping approach. In this approach, the substrate surface is first divided into a number of surface elements. If one DSMC parcel, which represents N_{eq} number of real molecules, has reacted with a surface element, then the corresponding number of sites will be marked as "reacted" and extracted from the list of available sites of the element. Thus, for a parcel that hits a surface element, the probability P_{rct} of it reacting with the element is

$$P_{rct} = f_i \cdot \gamma, \tag{2}$$

where γ is the sticking coefficient and f_i is the number fraction of unoccupied sites among the total number of sites in the i th surface element. Therefore, when $f_i = 0$, the surface element is completely saturated and no more DSMC parcels can react with the element. In the present study, the surface of the spherical particle is divided into 160 surface elements as shown in Fig. 2, such that each element has the same surface area and thus the same number of sites.

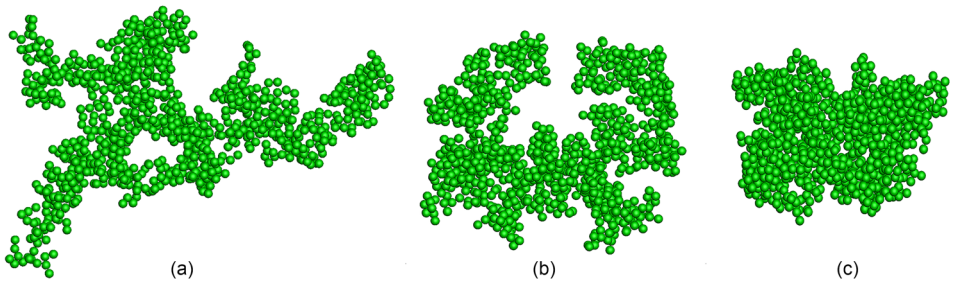

FIG. 1. (Color online) Numerically constructed fractal agglomerate with $k_f = 1.1$, $N = 1024$ for $D_f =$ (a) 2.1, (b) 2.3, and (c) 2.5.

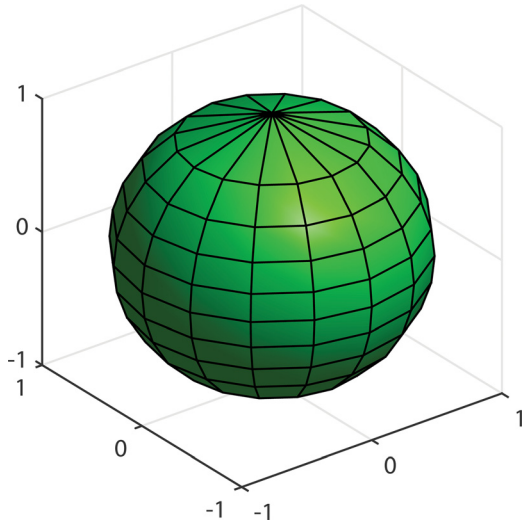

FIG. 2. (Color online) Surface of the nanoparticle is divided into 16×10 surface elements, each having the same surface area.

II. COMPUTATIONAL SETUP

We have made the computational domain a cuboid box large just enough to contain the constructed agglomerate. Our simulation results proved to be insensitive to the precise size of the box, with coating times increasing by less than 2% for a 20% larger box size. During the simulation, the precursor is released from the boundaries of the domain with a fixed concentration and allowed to react with the agglomerate surface. The gas phase in an ALD reactor is typically a mixture of different gas species, such as the precursors, carrier gas, and gaseous products. Although it is possible to include all these different gas species in a DSMC simulation, the aim of the present study is not to model one particular ALD process but rather to generically study the influence of fractal structure and gas rarefaction on the coating time. Therefore, we model the following generalized ALD half-cycle reaction:

$$A + \text{site (free)} \rightarrow \text{site (occupied)} + B, \tag{3}$$

where A is the precursor which is transported with an inert carrier gas C, and B is the gaseous product. We use identical molecular properties (those of Argon[32]) for all three gas species A, B, and C for the sake of the simplicity. The computational domain is initially filled with gas molecules of C, and as the simulation starts, A is introduced from the domain boundaries with a constant number fraction of 10%. The number density of surface sites is set to $\rho_{\text{site}} = 1.132 \times 10^{18}/\text{m}^2$. Precise values of sticking coefficients are rarely found in literature, in spite of the wide use of the concept. Moreover, the sticking coefficient strongly depends on the substrate material and the operating temperature, which makes it even harder to obtain consistent data from literature. Rose *et al.*[38] reported that the sticking coefficient of tetrakis(ethylmethylamino)hafnium on hydroxyl groups depends exponentially on the substrate temperature, rendering 0.56 at 270 °C. We adopt these values for the sticking coefficient and temperature in our modeling. For such a high sticking coefficient, reaction is fast compared to diffusion for large N, and as a result, coating times are rather insensitive to the precise value of γ. This was confirmed in our study by increasing γ from 0.56 to 1.0, leading to small changes in coating time for large N.

The simulated spherical nanoparticles have a diameter of $2a = 90$ nm. With these particles, a series of fractal agglomerates are constructed by varying N from 4 to 2048, D_f from 2.1 to 2.5, with $k_f = 1.1$. For each combination of N and D_f, one realization of the agglomerate was studied. To check the sensitivity to geometrical differences between different realizations, we studied three different realizations for $N = 128$ and $D_f = 2.5$. Once constructed, each agglomerate is embedded in one computational domain using the DSMC cut-cell method,[39,40] which allows each and every single particle to be fully resolved. In all the conducted simulations, we fulfil the common DSMC criteria[41,42] to ensure the accuracy of the results.

III. RESULTS AND DISCUSSION

A. Influence of pressure on coating time

ALD on particles can be carried out at low pressure[6] as well as at atmospheric pressure.[43] The amount of rarefaction, i.e., the ratio between the mean free path and pore size, increases for decreasing pressure. Therefore, we first study the influence of pressure. For a fixed agglomerate with $k_f = 1.1$, $N = 1024$, and $D_f = 2.5$, the pressure is varied from 0.22 to 2.0 bar ($\lambda = 562 \sim 61.8$ nm). The overall coating time is nondimensionalized with the time t_0 in which a surface element would be 99% coated when the precursor concentration at the surface would be the same as that of the domain boundaries. This reference time t_0 can be computed by solving the following differential equation:

$$-\rho_{\text{site}} \frac{df}{dt} = \frac{1}{4} u_t C_A \gamma f, \tag{4}$$

where ρ_{site} is the number density of surface sites, f is the number fraction of active sites, u_t is the molecular thermal velocity, and C_A is the precursor molecule number density. Equation (4) leads to the following expression for t_0:

$$t_0 = \frac{-\rho_{\text{site}}}{\frac{1}{4} u_t C_A \gamma} \ln(0.01), \tag{5}$$

which is of the order of 100 ns for 0.1 bar partial pressure of species A.

The choice of the length scale L in the definition of the Knudsen number is not obvious: an agglomerate is a multiscale structure with its smallest length scale being of the order of the particle radius a, and largest length scale being of the order of the overall agglomerate size R_g. To the best of our knowledge, it is not clear so far in literature what is the proper length scale for this particular problem. Therefore, we have simply chosen the particle radius a as the reference length scale and the gas mean free path is nondimensionalized into a Knudsen number by a. The molecular mean free path λ is computed from the variable soft sphere model as[32]

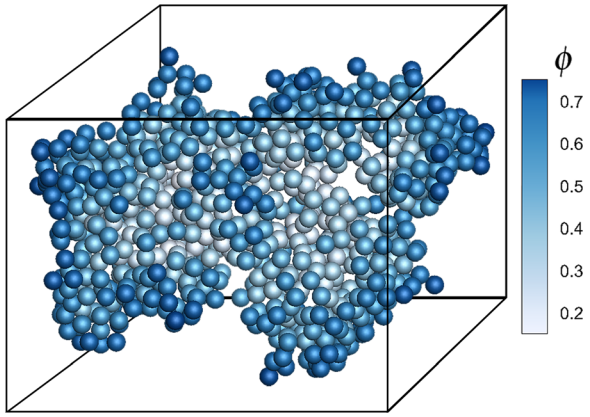

FIG. 3. (Color online) Surface coverage of each particle of the agglomerate, at $t = 0.65\,t_0$ for $P = 0.22$ bar. The cubic outline represents the computational domain.

$$\lambda = \frac{\alpha(5-2\omega)(7-2\omega)}{5(\alpha+1)(\alpha+2)} u_t \frac{\mu}{P} = \frac{k}{P}, \quad k = 0.01236\,\left(\mathrm{kg/s^2}\right), \tag{6}$$

where α is the exponent in the VSS model determined by the molecular properties, ω is the temperature exponent of viscosity, μ is the viscosity, and P is the pressure. As can be seen, λ is inversely proportional to P, and for the given range of P, it varies from $1.37a$ to $12.5a$.

Figure 3 shows the surface coverage of each particle of an agglomerate at time $t = 0.65\,t_0$ for $P = 0.22$ bar. It shows that the surface is not coated uniformly throughout the agglomerate. The outer particles are coated faster than the inner particles as can be expected intuitively. Figure 4 shows the overall surface coverage ϕ against the time t. As a reference case, a free molecular simulation is conducted by removing the molecular collisions from DSMC, i.e., $\lambda = \infty$. In general, when λ decreases, the overall coating time, normalized by that of a single particle, increases. The deviation from the free molecular results is only observable when λ is less than about $10a$. This suggests that for pressures below 0.1 bar, diffusion is well in the free molecular regime. Figure 5 shows the 99% overall saturation time $t_{99\%}$ against

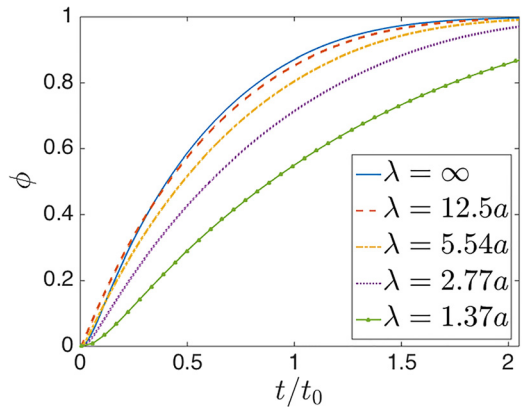

FIG. 4. (Color online) Overall surface coverage ϕ of the agglomerate against time t normalized by t_0. $\lambda = \infty$ denotes a free molecular simulation where the molecular collision is not taken into account.

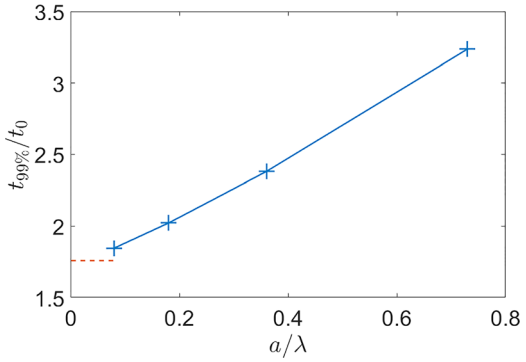

FIG. 5. (Color online) Saturation time of 99% $t_{99\%}$ normalized by t_0, against the particle radius a normalized by the gas mean free path λ. The red dashed line represents the normalized $t_{99\%}$ in the free molecular regime, i.e., $\lambda = \infty$.

the different λ. It again shows that the normalized coating time decreases with increasing λ, and for $\lambda = 12.5a$, the saturation time is very close to that in the free molecular flow.

B. Influence of agglomerate size on coating time

In this section, the pressure is fixed at 1 bar ($\lambda = 2.77a$), and agglomerates with different number of particles ($1 \leq N \leq 2048$) are simulated with $k_f = 1.1$ and $D_f = 2.5$.

Figure 6 shows the overall surface coverage ϕ against time t for agglomerates with different number of particles, in comparison with the analytic expression for ALD coating in the absence of diffusion limitations given in Eq. (4). The simulation results for $N = 1$ match very well with those analytic results, which indicates that for a single particle the system is well in the reaction-limited regime and can be accurately described by the analytic expression. As for the agglomerates, the overall coating time increases for increasing number of particles.

In order to analyze our results, and considering the resemblance between the gas diffusion in narrow holes and that in the pores of a porous agglomerate, we utilize the Gordon model,[44] which was developed to predict ALD coating times in narrow holes.

The Gordon model analyzes a self-limiting ALD surface coating reaction in a long, narrow, cylindrical hole or trench.

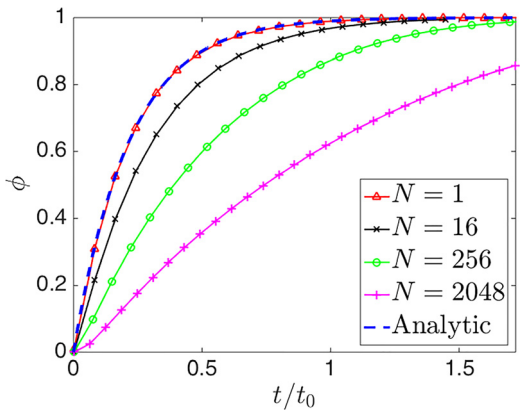

FIG. 6. (Color online) Overall surface coverage ϕ against time t normalized by t_0 for a single particle, in comparison with the analytic expression in Eq. (4).

As time progresses, the length of the coated part of the hole wall increases from the hole mouth downward. The increment of time dt needed for coating an additional length dl in the hole is computed from the balance between the local flux and consumption by the hole side walls, i.e.,

$$F(l)A_{\perp}(l)\cdot dt=\rho_{\text{site}}a_V(l)A_{\perp}(l)\cdot dl. \tag{7}$$

Here, $F(l)$ is the molecular precursor net flux entering the hole at depth l, $A_{\perp}(l)$ is the cross sectional area of the hole, ρ_{site} is the number of surface sites to be covered per unit area, and $a_V(l)$ is the wall surface area to be coated per unit volume of the hole. Thus, the total coating time T for the side walls of a hole of depth L is obtained as

$$T=\int_0^T dt=\rho_{\text{site}}\int_0^L\frac{1}{F(l)}a_V(l)dl. \tag{8}$$

In the Gordon model for a cylindrical hole with radius r_p, a_V is not a function of l and equal to $a_v=2/r_p$, and the precursor flux $F(l)$ inside the hole is expressed as a function of depth l as

$$F(l)=\frac{F_0}{1+c_{CL}\dfrac{l}{r_p}}, \tag{9}$$

with $F_0=(1/4)u_tC_A$ the molecular flux at the mouth of the hole. The denominator in Eq. (9) is called Clausing factor,[45] and it indicates how much the flux is reduced at a given depth l, compared to that at the entrance. The order 1 constant c_{CL} equals 3/8 for cylindrical holes, and varies for different hole cross sectional shapes.[46]

For quasispherical fractal agglomerates with $D_f>2$ and radius of gyration R_g, we now consider the above model in a spherical coordinate system, with its origin ($r=0$) defined at the center of mass of the agglomerate. Then, the coating penetration depth l is replaced by (R_g-r). In a fractal agglomerate, the amount of reactive surface per unit volume $a_V(r)$, as a function of radial position, is computed from

$$\begin{aligned}a_V(r)&=\frac{4\pi a^2dN}{4\pi r^2dr}=\frac{4\pi a^2k_fD_fa^{-1}\left(\dfrac{r}{a}\right)^{D_f-1}dr}{4\pi r^2dr}\\&=k_fD_fa^{2-D_f}r^{D_f-3}.\end{aligned} \tag{10}$$

This shows that in fractal agglomerates with $D_f<3$, $a_V(r)$ decreases with increasing r, as the agglomerate becomes less dense with increasing r.

The aspect ratio l/r_p of an agglomerate pore is estimated as

$$\begin{aligned}\frac{1}{r_p}l&=\frac{a_V}{2}(R_g-r)=\frac{4\pi a^2k_f\left(\dfrac{R_g}{a}\right)^{D_f}}{2\dfrac{4}{3}\pi {R_g}^3}(R_g-r)\\&=\frac{3}{2}k_fa^{2-D_f}{R_g}^{D_f-3}(R_g-r).\end{aligned} \tag{11}$$

By substituting Eqs. (10) and (11) into Eq. (8), and integrating from 0 to R_g, we get

$$\begin{aligned}t&=\int_0^t dt'=\frac{\rho_{\text{site}}}{F_0}\int_0^{R_g}\Big[k_fD_fa^{2-D_f}r^{D_f-3}\\&\quad+\frac{3}{2}c_{CL}k_f^2D_fa^{4-2D_f}\left({R_g}^{D_f-2}r^{D_f-3}-{R_g}^{D_f-3}r^{D_f-2}\right)\Big]dr\\&=\frac{\rho_{\text{site}}k_fD_f}{F_0}\left(\frac{1}{D_f-2}\left(\frac{R_g}{a}\right)^{D_f-2}\right.\\&\quad\left.+\frac{3}{2}c_{CL}\frac{k_f}{(D_f-1)(D_f-2)}\left(\frac{R_g}{a}\right)^{2D_f-4}\right),\end{aligned} \tag{12}$$

with Eq. (1), this can be rewritten as

$$\begin{aligned}t&=\frac{\rho_{\text{site}}}{F_0}\left[\frac{D_f}{D_f-2}{k_f}^{2/D_f}N^{D_f-2/D_f}+\frac{3}{2}c_{CL}\right.\\&\quad\left.\times\frac{D_f}{(D_f-2)(D_f-1)}{k_f}^{4/D_f}N^{2D_f-4/D_f}\right]\\&=k_1N^{D_f-2/D_f}+k_2N^{2D_f-4/D_f}.\end{aligned} \tag{13}$$

In the Gordon model for a hole, the coating time for the bottom wall is added to Eq. (8) as a separate term, which gives the asymptotic value of $t=t_0$ when $l=0$, i.e., when the hole depth is zero and deposition takes place on a flat surface. Similarly, in our model for deposition on a fractal agglomerate, this asymptotic value of $t=t_0$ should hold for $N=1$. Therefore, we add a similar additional term to Eq. (13) to fulfil this requirement as

$$t/t_0=k_1N^{D_f-2/D_f}+k_2N^{2D_f-4/D_f}+(1-k_1-k_2), \tag{14}$$

with

$$k_1=\frac{\rho_{\text{site}}}{F_0}\frac{1}{D_f-2}{k_f}^{2/D_f}D_f\frac{1}{t_0}=\frac{\gamma}{\ln(100)}\frac{1}{D_f-2}{k_f}^{2/D_f}D_f, \tag{15}$$

and

$$\begin{aligned}k_2&=\frac{3}{2}c_{CL}\frac{\rho_{\text{site}}}{F_0}\frac{1}{(D_f-2)(D_f-1)}{k_f}^{4/D_f}D_f\frac{1}{t_0}\\&=\frac{3}{2}c_{CL}\frac{\gamma}{\ln(100)}\frac{1}{(D_f-2)(D_f-1)}{k_f}^{4/D_f}D_f.\end{aligned} \tag{16}$$

The ratio k_1/k_2 depends on the geometrical properties of the agglomerate only, as

$$\frac{k_1}{k_2}=\frac{2}{3}\frac{1}{c_{CL}}(D_f-1){k_f}^{-2/D_f}. \tag{17}$$

Our model predicts that for fractal agglomerates with $2<D_f<3$ and large N [when the last term in Eq. (12) dominates] the coating time t scales less than quadratically with the size of the agglomerate R_g (for example, for $D_f=2.5$, t scales linearly with R_g). For nonfractal agglomerates

(i.e., $D_f = 3$) and large N, our model predicts that the coating time t scales quadratically with the size of the agglomerate R_g. This difference is due to the fact that for fractal agglomerates with $D_f < 3$ the porosity increases when moving away from the center, while for $D_f = 3$ the porosity is independent of radial position. It should be noted that for $D_f = 3$, our model is identical to the original Gordon model for a hole, which predicts a coating time proportional to the square of the hole depth.

For $D_f = 2.5$, Eq. (14) predicts $t/t_0 = k_1 N^{1/5} + k_2 N^{2/5} + (1 - k_1 - k_2)$. We fitted the constants k_1 and k_2 to simulated 99% saturation times $t_{99\%}$ for agglomerates with different number of particles ($1 \le N \le 2048$), $k_f = 1.1$ and $D_f = 2.5$, as shown in Fig. 7. As can be seen, the fitted curve matches the simulation data very well. It indicates that our generalized form of the Gordon model accurately predicts the scaling of the coating time of fractal agglomerates with increasing particle number. From our fitting to the data in Fig. 7, we find $k_1/k_2 = 2.16$, suggesting [with Eq. (17)] a value $c_{CL} = 0.43$ in the Clausing factor for $D_f = 2.5$, which appears to be a very reasonable value for our highly irregular pores.

With our above model, we can now estimate that for realistic fractal agglomerates with $N \sim 10^9$ and $D_f = 2.5$, the coating time would exceed that of a single particle by a factor of around 4000, as opposed to a factor 10^6 for a nonfractal agglomerate. This estimate, obviously, is highly sensitive to the precise value of the exponent in the second term on the rhs of Eq. (14), which we could not validate for very large N. Nevertheless, it is clear that the coating time for fractal agglomerates is orders of magnitude smaller than that of nonfractal agglomerates.

C. Influence of fractal dimension on coating time

In this section, the pressure is fixed at 1 bar, with $\lambda = 2.77a$, and the fractal dimension D_f is varied from 2.1 to 2.5 with $k_f = 1.1$ and $N = 1024$.

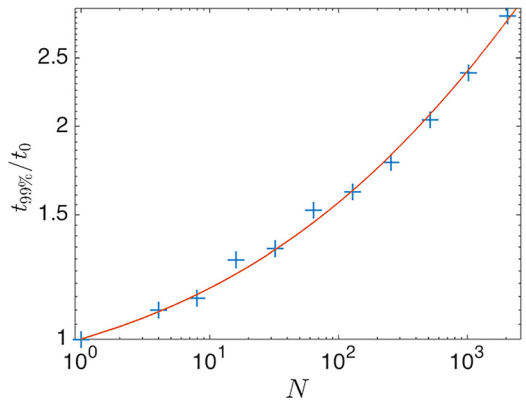

FIG. 7. (Color online) Saturation time of 99% $t_{99\%}$ normalized by t_0 against the number of particles N in an agglomerate. For $N = 128$, the saturation times for three different realizations of the agglomerates are shown, which are virtually identical. For all other N, only one realization is included. The red line represents a fitting according to Eq. (14) with $k_1 = 0.1414$ and $k_2 = 0.0655$.

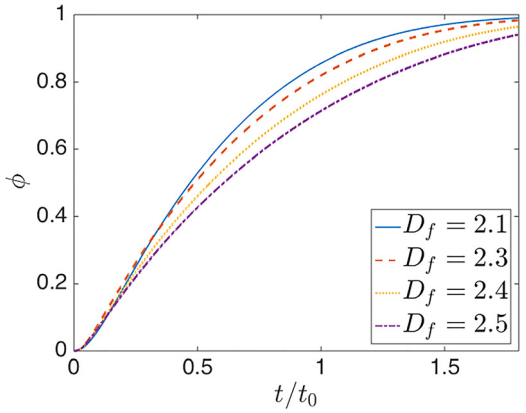

FIG. 8. (Color online) Overall surface coverage ϕ against time t normalized by t_0 for agglomerates with $k_f = 1.1$, $N = 1024$.

Figure 8 shows the overall surface coverage ϕ against time t for different fractal dimensions. In general, the coating time increases for increasing fractal dimension. We compare the simulated 99% saturation time $t_{99\%}$ with the analytic expression in Eq. (14). For $D_f < 2.5$, the values of k_1 and k_2 have been computed from the fitted values of k_1 and k_2 for $D_f = 2.5$, using Eqs. (15) and (16) in which C_{CL} was kept constant for all D_f. This comparison is shown in Fig. 9. As can be seen, the simulation results agree very well with our model for $D_f \ge 2.3$, while some deviations are observable for $D_f < 2.3$. This indicates that values of k_1 and k_2 obtained for large D_f are inaccurate for smaller D_f, probably due to (1) changes in pore shape, leading to different C_{CL}, (2) break down of the assumption of a quasispherical agglomerate shape with an average pore size depending on radial position only, rather than a fully three dimensional pore size distribution.

IV. SUMMARY AND CONCLUSIONS

We have developed a computational model for simulating atomic layer deposition on fractal nanoparticle agglomerates with fractal dimension $2 < D_f < 3$. This model accounts for a self-limiting ALD half cycle reaction and gas diffusion in

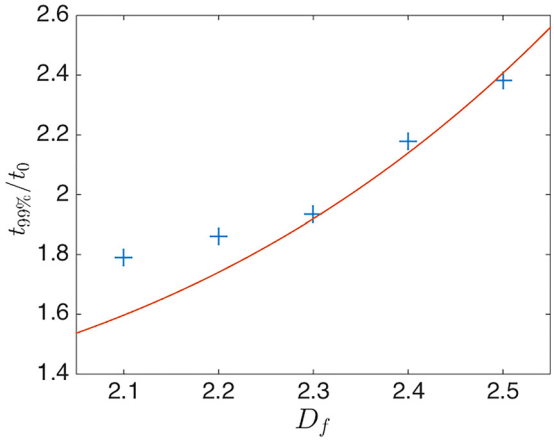

FIG. 9. (Color online) Saturation time of 99% $t_{99\%}$ normalized by t_0 against the fractal dimension D_f, for $k_f = 1.1$ and $N = 1024$. The red line represents the expression in Eq. (14), with the fitted k_1 and k_2 from Fig. 7.

the rarefied regime within a fully resolved fractal agglomerate of spherical nanoparticles. We also derived a generalized form of the Gordon model for ALD coating within a cylindrical hole or trench, which we extended to ALD coating within fractal geometries. Based on the present study with our model, we draw the following conclusions:

(1) The overall coating time of an agglomerate, normalized by that of a single particle, decreases for decreasing pressure, i.e., increasing gas mean free path λ, up to $\lambda \sim 10a$, whereas it becomes independent of pressure for $\lambda > 10a$, with a the nanoparticle radius. This indicates that a is the proper length scale for calculating the Knudsen number. For pressures below 0.1 bar, diffusion in the simulated agglomerates is well in the free molecular regime, and further reduction of the pressure has a little influence on the normalized coating time.
(2) The overall coating time increases as the number of particles of an agglomerate increases. Our generalization of the Gordon model predicts the required coating time of a large agglomerate to scale with the number of particles to the power $(2 - 4/D_f)$, in excellent agreement with simulation results for $D_f = 2.5$, This model predicts that realistic agglomerates of $O(10^9)$ nanoparticles require coating times that are 3–4 orders of magnitude larger than for a single particle.
(3) The overall coating time increases for increasing fractal dimension D_f in agreement with our generalized Gordon model. The two model constants in our model were found to slightly depend on the fractal dimension.

ACKNOWLEDGMENTS

This work was supported by NanoNextNL, a micro and nanotechnology consortium of the government of the Netherlands and 130 partners.

[1]J. Li, X. Liang, D. M. King, Y.-B. Jiang, and A. W. Weimer, Appl. Catal., B **97**, 220 (2010).
[2]A. Goulas and J. R. van Ommen, KONA Powder Part. J. **31**, 234 (2014).
[3]W. E. Bawarski, E. Chidlowsky, D. J. Bharali, and S. A. Mousa, Nanomed. Nanotechnol. Biol. Med. **4**, 273 (2008).
[4]J. W. Elam, N. P. Dasgupta, and F. B. Prinz, MRS Bull. **36**, 899 (2011).
[5]S. M. George, Chem. Rev. **110**, 111 (2010).
[6]L. F. Hakim, S. M. George, and A. W. Weimer, Nanotechnology **16**, S375 (2005).
[7]D. Valdesueiro, G. M. H. Meesters, M. T. Kreutzer, and J. R. van Ommen, Materials **8**, 1249 (2015).
[8]J. R. van Ommen, J. M. Valverde, and R. Pfeffer, J. Nanopart. Res. **14**, 737 (2012).
[9]L. de Martín, A. Fabre, and J. R. van Ommen, Chem. Eng. Sci. **112**, 79 (2014).
[10]L. de Martín, W. G. Bouwman, and J. R. van Ommen, Langmuir **30**, 12696 (2014).
[11]F. Grillo, M. T. Kreutzer, and J. R. van Ommen, Chem. Eng. J. **268**, 384 (2015).
[12]E. W. Thiele, Ind. Eng. Chem. **31**, 916 (1939).
[13]R. Krishna, J. Phys. Chem. C **113**, 19756 (2009).
[14]M.-O. Coppens and G. F. Froment, Chem. Eng. Sci. **50**, 1013 (1995).
[15]F. J. Keil, Catal. Today **53**, 245 (1999).
[16]F. J. Keil, Top. Curr. Chem. **307**, 69 (2012).
[17]M. Sahimi, G. R. Gavalas, and T. T. Tsotsis, Chem. Eng. Sci. **45**, 1443 (1990).
[18]J. A. H. Dreyer, N. Riefler, G. R. Pesch, M. Karamehmedović, U. Fritsching, W. Y. Teoh, and L. Mädler, Chem. Eng. Sci. **105**, 69 (2014).
[19]G. L. Vignoles, J. Phys. IV France **5**, C5-159 (1995).
[20]N. Reuge and B. Caussat, Chem. Vap. Deposition **17**, 305 (2011).
[21]A. M. Lankhorst, B. D. Paarhuis, H. J. C. M. Terhorst, P. J. P. M. Simons, and C. R. Kleijn, Surf. Coat. Technol. **201**, 8842 (2007).
[22]E. Chassaing and B. Sapoval, J. Electrochem. Soc. **141**, 2711 (1994).
[23]P. Meakin and B. Sapoval, Phys. Rev. A **43**, 2993 (1991).
[24]D. S. Grebenkov, M. Filoche, and B. Sapoval, Fractals **15**, 27 (2007).
[25]G. R. Pesch, N. Riefler, U. Fritsching, L. Colombi Ciacchi, and L. Mädler, AIChE J. **61**, 2092 (2015).
[26]J. Dendooven, D. Deduytsche, J. Musschoot, R. L. Vanmeirhaeghe, and C. Detavernier, J. Electrochem. Soc. **156**, P63 (2009).
[27]H. C. M. Knoops, E. Langereis, M. C. M. van de Sanden, and W. M. M. Kessels, J. Electrochem. Soc. **157**, G241 (2010).
[28]M. Rose and J. W. Bartha, Appl. Surf. Sci. **255**, 6620 (2009).
[29]S. K. Friedlander, *Smoke, Dust, and Haze—Fundamentals of Aerosol Dynamics* (Oxford University, Oxford, 2000).
[30]A. V. Filippov, M. Zurita, and D. E. Rosner, J. Colloid Interface Sci. **229**, 261 (2000).
[31]K. Skorupski, J. Mroczkaa, T. Wriedt, and N. Riefler, Physica A **404**, 106 (2014).
[32]G. A. Bird, *Molecular Gas Dynamics and the Direct Simulation of Gas Flows* (Oxford University, New York, 1994).
[33]E. S. Oran, C. K. Oh, and B. Z. Cybyk, Annu. Rev. Fluid Mech. **30**, 403 (1998).
[34]Z.-C. Hong, C.-E. Zhen, and C.-Y. Yang, Numer. Heat Transfer, A **54**, 293 (2008).
[35]H. Akhlaghi, E. Roohi, and S. Stefanov, Int. J. Therm. Sci. **59**, 111 (2012).
[36]G. A. Bird, Comput. Math. Appl. **35**, 1 (1998).
[37]M. Ritala, M. Leskela, L. Niinisto, and P. Haussalo, Chem. Mater. **5**, 1174 (1993).
[38]M. Rose, J. W. Bartha, and I. Endler, Appl. Surf. Sci. **256**, 3778 (2010).
[39]C. Zhang and T. E. Schwartzentruber, Comput. Fluids **69**, 122 (2012).
[40]M. C. Lo, C. C. Su, J. S. Wu, and F. A. Kuo, Comput. Fluids **101**, 114 (2014).
[41]A. L. Garcia and W. Wagner, Phys. Fluids **12**, 2621 (2000).
[42]Z.-X. Sun, Z. Tang, Y.-L. He, and W.-Q. Tao, Comput. Fluids **50**, 1 (2011).
[43]R. Beetstra, U. Lafont, J. Nijenhuis, E. M. Kelder, and J. R. van Ommen, Chem. Vap. Deposition **15**, 227 (2009).
[44]R. G. Gordon, D. Hausmann, E. Kim, and J. Shepard, Chem. Vap. Deposition **9**, 73 (2003).
[45]P. Clausing, J. Vac. Sci. Technol. **8**, 636 (1971).
[46]P. J. Lobo, F. Becheri, and J. Gómez–Goñi, Vacuum **76**, 83 (2004).